Scientific Research Publishing

World Journal of Condensed Matter Physics, 2023, 13, 79-89
https://www.scirp.org/journal/wjcmp
ISSN Online: 2160-6927
ISSN Print: 2160-6919

A Dynamical Approach to the Explanation of the Upper Critical Field Data of Compressed H_3S

Gulshan Malik[1], Vijaya S. Varma[2]

[1]Theory Group, School of Environmental Sciences, Jawaharlal Nehru University, New Delhi, India
[2]Department of Physics and Astrophysics, University of Delhi, Delhi, India
Email: gulshanpmalik@yahoo.com, varma2@gmail.com

How to cite this paper: Malik, G. and Varma, V.S. (2023) A Dynamical Approach to the Explanation of the Upper Critical Field Data of Compressed H_3S. *World Journal of Condensed Matter Physics*, **13**, 79-89.
https://doi.org/10.4236/wjcmp.2023.133005

Received: May 10, 2023
Accepted: July 3, 2023
Published: July 6, 2023

Abstract

Excellent fits were obtained by Talantsev (MPLB 33, 1950195, 2019) to the temperature (T)-dependent upper critical field ($H_{c2}(T)$) data of H_3S reported by Mozaffari et al. [Nature Communications 10, 2522 (2019)] by employing four alternative phenomenological models, each of which invoked two or more properties from its sample-specific set S_1 = {T_c, gap, coherence length, penetration depth, jump in sp.ht.} and a single value of the effective mass (m^*) of an electron. Based on the premise that the variation of $H_{c2}(T)$ is due to the variation of the chemical potential $\mu(T)$, we report here fits to the same data by employing a T-, μ- and m^*-dependent equation for $H_{c2}(T)$ and three models of $\mu(T)$, viz. the linear, the parabolic and the concave-upward model. For temperatures up to which the data are available, each of these provides a good fit. However, for lower values of T, their predictions differ. Notably, the predicted values of $H_{c2}(0)$ are much higher than in any of the models dealt with by Talantsev. In sum, we show here that the addressed data are explicable in a framework comprising the set S_2 = {μ, m^*, interaction parameter λ_m, Landau index N_L}, which is altogether different from S_1.

Keywords

Compressed H_2S, Upper Critical Magnetic Field, Pairing Equation Incorporating Temperature, Chemical Potential and Magnetic Field, Temperature Dependence of the Chemical Potential

1. Introduction

1.1. Preamble

The discovery by Drozdov *et al.* [1] of H_2S as a superconductor (SC) having a critical temperature (T_c) of ≈ 200 K at the ultra-high pressure of ≈ 150 GPa in

2015 is a significant landmark in the more than a century long quest for room temperature superconductivity. Understandably therefore a huge effort—experimental as well as theoretical—has been expended in the intervening years to unravel various features of this SC, which has led to some valuable insights and concrete results; for a partial summary of these, see [2]. In this paper, we concern ourselves with the temperature-dependent upper critical field ($H_{c2}(T)$) of compressed H_2S not only because it sheds light on some conceptual aspects of its superconductivity, but also because it is an important property from the point of view of its practical usage.

1.2. Earlier Work Dealing with the $B_{c2}(T)$ of Compressed H_2S

In a recent paper, Talantsev [3] obtained excellent fits to the temperature (T)-dependent upper critical field B_{c2} data of highly compressed H_3S reported by Mozaffari *et al.* [4] by employing the following four models:

1) The Baumgartner-Werthamer-Helfand-Hohenberg (B-WHH) model

This model is based on the following relation given by Werthamer, Helfand and Hohenberg [5]

$$\ln\left(\frac{T}{T_c(B=0)}\right)=\psi\left(\frac{1}{2}\right)-\psi\left(\frac{1}{2}+\frac{\hbar DB_{c2}(T)}{2\phi_0 kT}\right), \tag{1}$$

where Ψ is the Euler psi-function or the digamma function, T_c is the critical temperature, D is the diffusion constant for the normal electrons/holes in the conduction band, $\phi_0=2.07\times10^{-15}$ Wb is the flux quantum and k the Boltzmann constant. This relation has two free fitting parameters viz., $T_c(B=0)$ and D. In a modification of (1) where the free parameter D is replaced by $\xi(0)$—the coherence length at $T=0$, Baumgartner *et al.* [6] proposed a relation which has been found to be quite accurate. Designated above as the B-WHH model, this relation is

$$B_{c2}(T)=\frac{\phi_0}{1.386\pi\xi^2(0)}\left[(1-t)-0.153(1-t)^2-0.152(1-t)^4\right], \tag{2}$$

where $t=T/T_c$ is the reduced temperature.

2) The Jones-Hulm-Chandrasekhar model [7]

$$B_{c2}(T)=B_c(T)\frac{\sqrt{2}\lambda(0)}{1.77\xi^2(0)}\left(\frac{1-t^2}{1+t}\right), \tag{3}$$

where $B_c(T)$ is the thermodynamic critical field and $\lambda(0)$ is the London penetration depth at $T=0$.

3) The Gor'kov model [8] as recast in [3]

$$B_{c2}(T)=\frac{\phi_0}{3.54\pi\xi^2(0)}\left(1.77-0.43t^2+0.07t^4\right)\left(1-t^2\right). \tag{4}$$

4) The tribrid model

We have named the fourth model in [3] as the tribrid model because it is

based on the Gorter-Casimir two-fluid theory, the Ginsberg-Landau theory and the BCS theory. This model employs the following equation

$$B_{c2}(t)=\frac{\phi_0}{2\pi\xi^2(0)}\left[F_1(t)F_2(t)\right], \tag{5}$$

where

$$F_1(t)=\left(\frac{1.77-0.43\,t^2+0.07\,t^4}{1.77}\right)^2$$

and

$$F_2(t)=\left[1-\frac{1}{2k\;t\;T_c}\int_0^\infty \mathrm{d}\varepsilon/\cosh^2\left(\frac{\sqrt{\varepsilon^2+\Delta^2(t\;T_c)}}{2k\;t\;T_c}\right)\right]^{-1}.$$

Talantsev's work [3] relates the empirical B_{c2}(T) data of H_3S with the set of four of its fundamental parameters, viz., T_c, $\xi(0)$, $\Delta(0)$ and $\Delta C/C$, where $\Delta(0)$ is the gap of the SC at $T=0$ and $\Delta C/C$ is the jump in its electronic specific heat at $T=T_c$.

1.3. The Rationale and the Scope of the Present Work

It seems apt to label the four models described above as *phenomenological* because they are not directly based on the *dynamical* variables of the problem as, for example, λ_m, the magnetic interaction parameter. In this paper, we meet the need to explain the $B_{c2}(T)$ data reported in [4] as dealt with in [3] via a dynamical equation for pairing that incorporates the chemical potential μ, T and the applied magnetic field H—it being our basic premise that the Fermi energy (E_F) or μ plays a fundamental role in determining the properties of a superconductor, regardless of its size, shape and the manner of preparation all of which determine its E_F at $T=0$ or μ when $T\neq 0$. This equation and the procedure for solving it are given in the next section. A notable feature of our approach is that it sheds light on a set of parameters corresponding to any value of $H_{c2}(T)$, which is altogether different from the set of parameters on which the study reported in [3] was based.

2. The Pairing Equation Incorporating Chemical Potential, Temperature and an Applied Field

Incorporating temperature, chemical potential and an applied field, the generalized BCS equation derived in [9] and employed here is

$$\begin{aligned}\mathrm{Eq1}(t,h)&\equiv 1-2\lambda_m\int_{L_1(\rho)}^{L_2(\rho)}\mathrm{d}z\sum_{n=0}^{N_L(\hbar)}\frac{\tanh\left[\left(\mu/2k\;t\;T_c\right)\left\{z^2-1+\left(n+1/2\right)\hbar\;\Omega\left(h,\eta\right)/\mu\right\}\right]}{z^2-1+\left(n+1/2\right)\hbar\;\Omega\left(h,\eta\right)/\mu}\\&=0\end{aligned} \tag{6}$$

where

$$\rho = \mu/k\theta,\ L_1(\rho) = \sqrt{(\rho-1)/3\rho},\ L_2(\rho) = \sqrt{(\rho+1)/3\rho},\ \Omega(h) = \Omega_0 h H_{c2}(0)/\eta$$

$$\Omega_0 = e/mc,\ h = H/H_{c2}(0),\ N_L(h,\rho) = floor\left[\frac{2k\theta(\rho+1)}{3\hbar\Omega(h)} - \frac{1}{2}\right],$$

and θ is the Debye temperature (DT) of the ions that cause pairing, $\eta = m^*/m$ (m^*= effective mass of an electron and m = the free electron mass) and $N_L(h)$ is the Landau index. We have used the symbol H_{c2} above in lieu of B_{c2} in [1] because (6) has been obtained by employing the units commonly employed in the BCS theory, e.g., Gauss for the magnetic field.

3. Addressing the $H_{c2}(T)$ Data reported by Mozaffari *et al.* [4] via Equation (6)

3.1. The Debye Temperature of the Ions Responsible for Pairing and a Generic Model for the Variation of the Chemical Potential with Temperature

1) In order to deal with the above data, we first need to fix the value of θ to be used in (6). Given that H_3S is believed to result when H_2S is subjected to ultra-high pressure via the reaction $2H_2S \rightarrow (H_3S)^+ + (HS)^-$ [10] and that $\theta(H_3S)$ = 1531 K [11], we need to resolve $\theta(H_3S)$ into the DTs of the H and the S ions because the two gaps of H_3S have been explained by invoking the 2-phonon exchange mechanism due to these ions [2]. Employing the double-pendulum model [12], we have

$$\theta_H = 1983.2 \text{ K},\ \theta_S = 174.5 \text{ K}. \tag{7}$$

We note that both of these DTs are *needed* [2] for an explanation of the empirical value of the T_c of H_3S and its inferred gap-values of about 40 meV and 28 meV because the 1-phonon exchange mechanism (1PEM) per se due either to the H or the S ions violates the Bogoliubov constraint [13]. Since a magnetic field considerably weakens the strength of the interaction, it turns out—as will be seen—that the data being addressed here are attributable to the interactions caused by the H ions alone.

2) With θ fixed as θ_H as in (7), we obtain via (6) the value of λ_m at $T = T_c$, *i.e.*, t = 1. For this purpose, we need to specify the values of H_{c2} at t = 1, ρ (since $\mu = \rho k\theta$) and η. This is done as follows. We employ H_{c2} (1) = 300 G, which is the self-field that remains even when there is no applied field; ρ = 1, *i.e.*, $\mu = k\theta_H$ = 170.9 meV, which is in accord with the estimate of the E_F of H_3S given by Gor'kov and Kresin as $500 \geq E_F \geq 100$ (meV) [14], and η = 2.76 because this is the value employed in [3]. The effect of the values of ρ and η other than these will be addressed below.

3) As per our premise in Section 1.2, we now need to specify how μ varies with t between 1 and 0. We note in this context that the t-dependent values of the critical current density (j_c) of H_3S have recently been explained by making in an equation similar to (6) and the number equation the following replace-

ments:

$$\mu \to q(T)\mu,\ \lambda_m \to \lambda_m \Big/ \sqrt{q(t)} \quad [15].$$

Observing that the form of $h_{c2}(t)$ is predominantly determined by the form of $\lambda_m(t)$ and that a good phenomenological description for the variation of the former is provided by $h_{c2}(t) = \left(1 - t^2\right)$, we assume that

$$\mu(t) = \mu(1)q(t),\ \lambda_m(t) = \lambda_m(1)q(t), \tag{8}$$

and

$$q(t) = 1 + a_0\left(1 - t^{a1}\right)^{a2}. \tag{9}$$

Remarks:

a) It seems pertinent to note that a model is needed to extend or supplement the experimental data up to 0 K because such data are available only up to T ≈ 100 K, which depends on the size of the sample. This is so, because the size of the sample is necessarily small—diameter ≈ 50 μm and thickness ≈ a few μm—in order to subject them to the desired high pressure in a diamond anvil cell. It has so far not been possible to cool such samples up to 0 K.

b) Note that regardless of the values of a_0, a_1 and a_2, $q(t) = 1$ for $t = 1$ whence $\mu(t)$ and $\lambda_m(t)$ in (8) reduce to their respective values at $t = 1$. In the following we deal with the empirical data by employing three models of $q(t)$ distinguished by the values of the constants in (9).

3.2. Three alternative Scenarios

We now illustrate the above procedure by considering the data-sets of two samples in [4].

Sample 1

The raw data for this sample comprise 23 values of $H_{c2}(T)$ for $105.1 \le T \le 191$ K. With

$$\theta = 1983.2,\ \rho = 1\left(\mu(1) = 170.9 \text{ meV}\right),\ \eta = 2.76,\ T_c = 191,\ H_{c0} = 100 \times 10^4 \text{ G}$$
$$t = 191/T_c = 1,\ h = 300/H_{c0},$$

the solution of (6) yields

$$\lambda_m(1) = 1.1281 \times 10^{-6}. \tag{10}$$

The value of $H_{c0} \equiv H_{c2}(0)$ (an unknown) noted above has been chosen as a matter of convenience because it enables us to look for the solutions by varying h between 0 and ≈ 1.

We note that our results of course do not depend on the choice of the value of H_{c0} and that this step which yields (10) is common to all the three forms of $q(t)$ dealt with below.

1) The linear form of $q(t)$

If in the generic form of $q(t)$ in (9) we let $a_1 = a_2 = 1$, then we obtain the linear form of $q(t)$, viz.,

$$q_1(a_0, t) = 1 + a_0(1 - t).$$

As noted in (8), this is the factor via which we cause μ to vary with t. Since $\mu = \rho k \theta$, we need to replace ρ in (6) by ρ times $q(a_0, t)$, whence

$$Eq1(t,h) \to Eq1(a_o,t,h),$$

$$L_1(\rho) \to L_3(\rho,a_0,t) = \sqrt{\frac{q_1(a_0,t)\rho - 1}{3q_1(a_0,t)\rho}},\ L_2(\rho) \to L_4(\rho,a_0,t) = \sqrt{\frac{q_1(a_0,t)\rho + 1}{3q_1(a_0,t)\rho}}$$

$$N_L(h,\rho) \to N_L(h,\rho,a_0,t) = floor\left[\frac{2k\theta\left[q_1(a_0,t)\rho + 1\right]}{3\hbar\Omega(h)} - \frac{1}{2}\right]. \quad (11)$$

To fix a_0, we need the input of one (t, h) point from the data under consideration. Choosing a value of t in the mid-range of the data, *i.e.*,

$$t = 150/T_c,\ h = 26.47\times10^4/H_{c0}. \quad (12)$$

We obtain

$$a_0 = 2165.4. \quad (13)$$

We can now employ (11) to calculate the value of h corresponding to any t. We do so for 16 points between $t = 1$ ($T = 191$ K) and 0 and obtain the limiting values of the parameters of interest as:

$$H_{c0} = 601.1\times10^4 \text{ G; for } 1 \ge t \ge 0\text{: } 0.171 \le \mu(t) \le 370.2 \text{ (eV)};$$
$$1.128\times10^{-6} \le \lambda_m(t) \le 2.444\times10^{-3};\ 1.811\times10^5 \ge N_L(t) \ge 9.793\times10^3. \quad (14)$$

The plot obtained for the variation of $H_{c2}(T)$ for all the 16 points in the range $191 \ge T \ge 0$ (K) is given below (Figure 1).

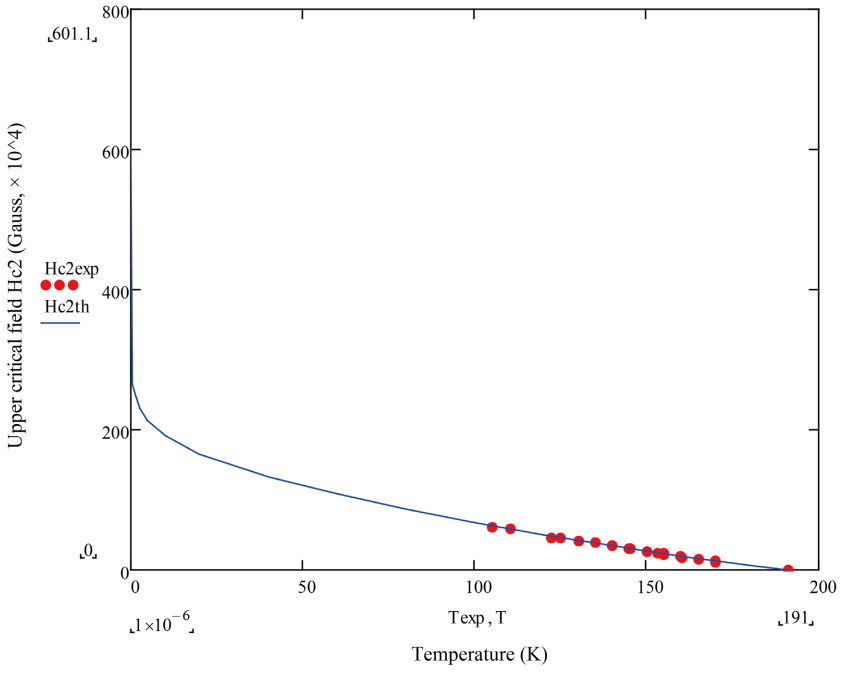

Figure 1. Plot of $H_{c2}(T)$ of compressed H_3S obtained via (6), (8) and the linear form of $q(t)$ noted in (11) for the sample for which $T_c = 191$ K. The filled circles denote the empirical values given in [2].

2) The "parabolic" form of $q(t)$

Let $a_1 = 2$ in (9), then

$$q_2(t) = 1 + a_0\left(1 - t^2\right)^{a_2}, \tag{15}$$

whence

$$Eq1(t,h) \to Eq1(a_0, a_2, t, h),$$

$$L_1(\rho) \to L_3(\rho, a_0, a_2, t) = \sqrt{\frac{q_2(a_0, a_2, t)\rho - 1}{3q_2(a_0, a_2, t)\rho}},\ L_2(\rho) \to L_4(\rho, a_0, a_2, t)$$

$$N_L(h, \rho) \to N_L(h, \rho, a_0, a_2, t),$$

where L_4 and N_L are given by the expressions for them as in (11) with $q_1(a_0, t)$ replaced by $q_2(a_0, a_2, t)$.

We now need the input of two (t, h) points from the empirical data to fix a_0 and a_2 by simultaneously solving Eq1(a_0, a_2, t_1, h_1) and Eq1(a_0, a_2, t_2, h_2). Choosing (t_1, h_1) and (t_2, h_2) as

$$\left(t_1 = 145/T_c,\ h_1 = 30.27\times 10^4/H_{c0}\right),\ \left(t_2 = 105.1/T_c,\ h_2 = 61.49\times 10^4/H_{c0}\right), \tag{16}$$

we obtain

$$a_0 = 1475.0,\ a_2 = 1.208. \tag{17}$$

These lead to the limiting values of the parameters of interest as:

$$\begin{aligned} &H_{c0} = 242.9\times 10^4 \text{ G; for } 1 \ge t \ge 0:\ 0.171 \le \mu(t) \le 252.2 \text{ (eV)},\\ &1.128\times 10^{-6} \le \lambda_m \le 1.665\times 10^{-3},\ 1.811\times 10^5 \ge N_L \ge 1.652\times 10^4. \end{aligned} \tag{18}$$

The plot now obtained for the variation of $H_{c2}(T)$ for 15 points in the range $191 \ge T \ge 0$ (K) is given below (**Figure 2**).

3) The concave-upward form of $q(t)$

For $a_2 = 1$ in (9), we have

$$q(t) = 1 + a_0\left(1 - t^{a_1}\right), \tag{19}$$

whence we again need to solve two simultaneous equations, viz., Eq1(a_0, a_1, t_1, h_1) and Eq1(a_0, a_1, t_2, h_2), in order to fix a_0 and a_1 with the input of two (t, h) points from the empirical data. Choosing the values of (t_1, h_1) and (t_2, h_2) as

$$\left(t_1 = 125/T_c,\ h_1 = 44.77\times 10^4/H_{c0}\right),\ \left(t_2 = 105.1/T_c,\ h_2 = 61.49\times 10^4/H_{c0}\right), \tag{20}$$

we obtain

$$a_0 = 2195.1,\ a_1 = 0.9549. \tag{21}$$

The limiting values of the parameters of interest now are:

$$\begin{aligned} &H_{c0} = 579.0\times 10^4 \text{ G; for } 1 \ge t \ge 0:\ 0.171 \le \mu(t) \le 252.2 \text{ (eV)},\\ &1.128\times 10^{-6} \le \lambda_m(t) \le 2.477\times 10^{-3},\ 1.811\times 10^5 \ge N_L(t) \ge 1.031\times 10^4 \end{aligned} \tag{22}$$

and the plot obtained for the variation of $H_{c2}(T)$ for 17 points in the range $191 \ge T \ge 0$ (K) is as given below (**Figure 3**).

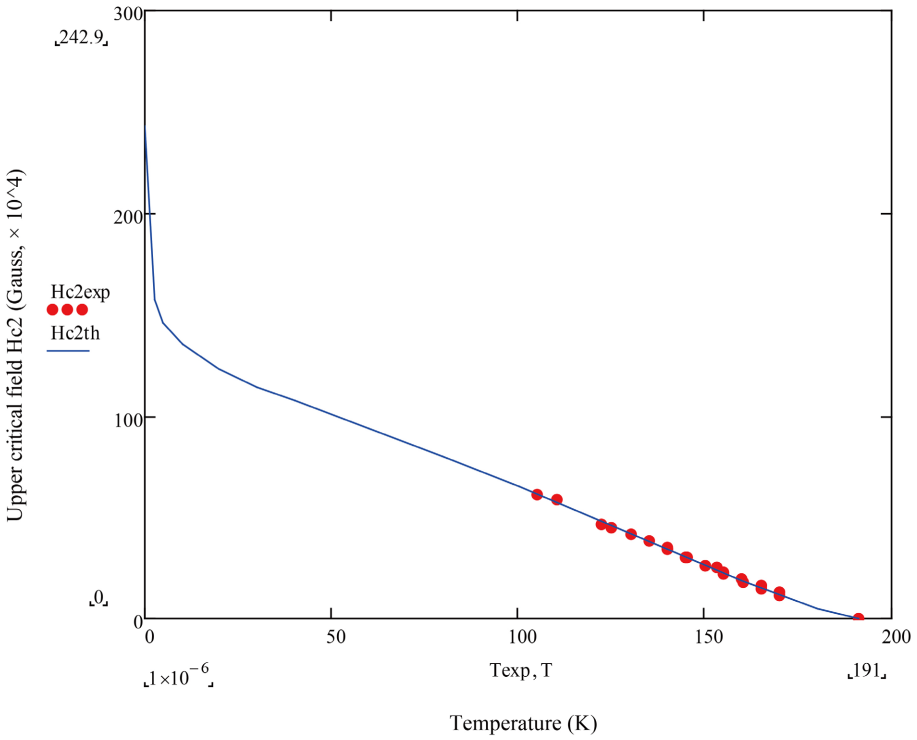

Figure 2. Plot of $H_{c2}(T)$ of compressed H_3S obtained via (6), (8) and the parabolic form of $q(t)$ noted in (15) for the sample for which T_c = 191 K. The filled circles denote the empirical values given in [2].

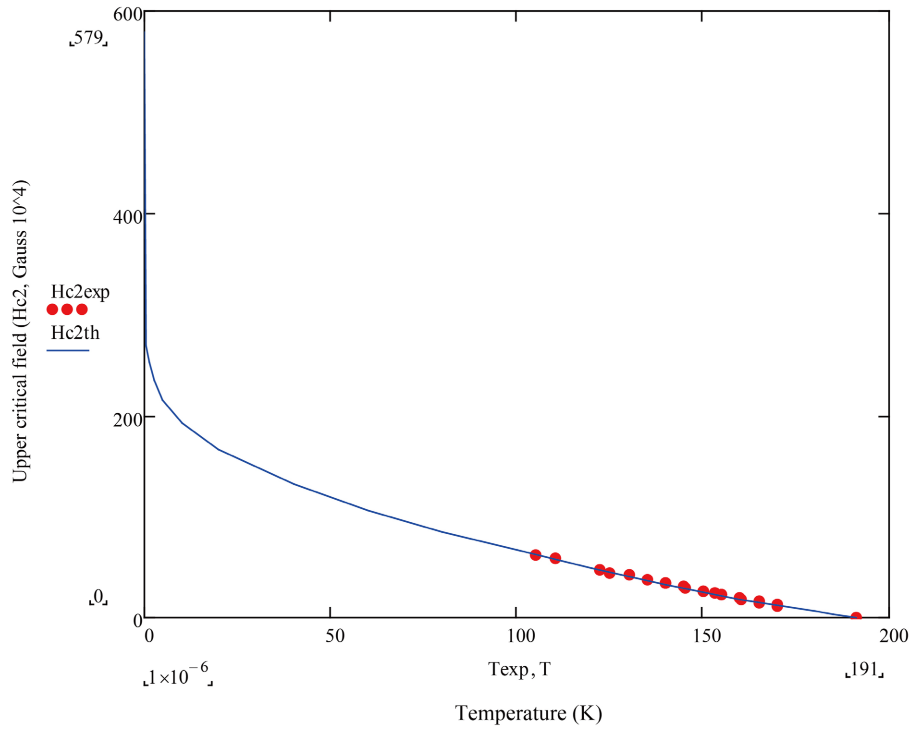

Figure 3. Plot of $H_{c2}(T)$ of compressed H_3S obtained via (6), (8) and the concave-upward form of $q(t)$ noted in (19) for the sample for which T_c = 191 K. The filled circles denote the empirical values given in [2].

Sample 2

The raw data for this sample comprise 24 values of $H_{c2}(T)$ for $55.9 \leq T \leq 173.7$ K. With the same values of θ, ρ and η, the plots of the variation of $H_{c2}(T)$ for this sample are similar to those for Sample 1 and are hence not given.

3.3. The Effect of Changing the Values of the Chemical Potential and the Effective Mass of the Electron

For both the samples dealt with above, the values of ρ and η employed for each of the three forms of q(t) were 1 and 2.76, respectively. Repeating the above exercise for any form of $q(t)$ with different values of ρ and η, e.g., $\rho = 1$, $\eta = 2.25$, 3.25, 4.0 and $\rho = 2$, $\eta = 2.76$, we found that while the values of a_0, a_1, etc., were now different, the plots of $H_{c2}(T)$ that we were led to were almost indistinguishable from the corresponding plots that we had obtained earlier.

4. Discussion and Conclusion

The fits to the empirical values of $h_{c2}(t)$ of several samples reported in [4] were obtained in [3] by employing a single value of $\eta = 2.76$ and four alternative phenomenological models, each of which invoked two or more properties from the following sample-specific set of the SC: $S_1 = \{T_c, \Delta(0), \xi(0), \lambda(0), \Delta C/C\}$. In this paper we have dealt with two of these samples and shown that the empirical data corresponding to them are also explicable by assuming that the variation of h_{c2} with t is caused predominantly by the variation of μ with t. This has been done by employing a μ-, H- and T-dependent equation [9] and three models for the variation of $\mu(t)$. We thus found that up to the lowest temperatures in the data sets (105.1 K for Sample 1; 55.09 K for Sample 2), each of these models provides an almost equally good fit, which is also in accord with the fits obtained in [3]. However, for lower temperatures, the predictions of the values of H_{c2} at $t = 0$ of these models differ significantly not only from each other, but also from the corresponding values in [3]. We also found that the assumed value of $\rho = 1$ (*i.e.*, $\mu = 170.9$ meV) at $t = 1$ and $\eta = 2.76$ are not unique in explaining the addressed data. Specifically, while $\rho = 2$ and $\eta = 2.25$, 2.76 or 3.25 also lead to good fits, the values of H_{c0} and $\mu(0)$ that one now obtains are even greater than their respective values for $\rho = 1$ and the same values of η. The set of properties with which we have related the empirical values of $H_{c2}(t)$ is: $S_2 = \{\mu, m^*$, interaction parameter λ_m, Landau index $N_L\}$, which is altogether different from S_1.

The rather high values of H_{c0} and $\mu(0)$ that we have been led to—vide (14), (18) and (22)—warrant an explanation, even if one chooses to ignore the linear model because of the *intuitive* feeling that it leads to *implausible* values of these parameters. We note in this context that the values of H_{c0} and $\mu(0)$, etc., noted above must be regarded as implicitly dependent on pressure, because they have been obtained with the input of the so-dependent empirical values of $H_c(t)$. There is a need therefore to ask as to how μ varies with T and pressure p, which leads us to draw attention to the kinetics of the chemical reactions where such

variations have been adequately investigated. For gaseous materials, in particular, it is well known that μ generally *increases* rapidly when ρ *increases* and that it *falls* steeply when T *increases*. So, μ depends rather sensitively on both T and p. The system we are concerned with in this paper is supposed to be subject to a constant ultra-high pressure and therefore, in analogy with the kinetics of the chemical reactions, ought to be characterized by a high value of μ at $T = 0$—which is what we have found for the Fermi gas model employed by us. On the other hand, although p for the system is maintained at the same high value, we have found that the increase in the value of T from 0 to $T_c = 191$ K causes μ to decrease to a value which is several orders of magnitude lower than its value at $T = 0$—which is also in accord with the kinetics of the chemical reactions.

In a recent paper and references therein, Hirsch and Marsiglio [16] have raised the important issue of whether or not H_3S is a genuine SC because, according to them, it does not satisfy the criterion of exhibiting the Meissner effect. It seems to us that this provocative issue can also be addressed via the considerations of this paper by adopting a variant of the template provided by Dogan and Cohen [17], which we propose to do in another paper.

We conclude by noting that the approach based on a T-dependent Bethe-Salpeter equation employed here for an explanation of the empirical $H_{c2}(T)$ values has—with appropriately chosen kernels—also been employed earlier for a dynamical explanation of such diverse phenomena as the solar emission lines, vide [18] and references therein, and the quarkonium mass spectra, vide [19] and references therein. This should not be surprising because each of these phenomena is concerned with a bound state problem in a medium at finite temperature: solar emission lines with the bound states of all kinds of ions in various stages of ionization, spectra of mesons with the bound states of appropriate quarks, and superconductivity with the bound states of electrons.

Conflicts of Interest

The authors declare no conflicts of interest regarding the publication of this paper.

References

[1] Drozdov, A.P., Eremets, M.I, Troyan, I.A., Ksenoafontov, V. and Shylin, S.I. (2015) Conventional Superconductivity at 203 Kelvin at High Pressure in Sulfur Hydride System. *Nature*, **525**, 73-76. https://doi.org/10.1038/nature14964

[2] Malik, G.P. (2022) Superconductivity of Compressed H_2S in the Framework of the Generalized BCS Equations. *European Physics Journal Plus*, **137**, Article No. 786. https://doi.org/10.1140/epjp/s13360-022-03003-z

[3] Talantsev, E.F. (2019) Classifying Superconductivity in Compressed H_3S. *Modern Physics Letters B*, **33**, 19501951. https://doi.org/10.1142/S0217984919501951

[4] Mozaffari, S., *et al.* (2019) Superconducting Phase Diagram of H_3S under High Magnetic Fields. *Nature Communications*, **10**, 2522. https://doi.org/10.1038/s41467-019-10552-y

[5] Werthamer, N.R., Helfand, E. and Hohenberg, P.C. (1966) Temperature and Purity Dependence of the Superconducting Critical Field, H_{c2}. III Electron Spin and Spin-Orbit Effects. *Physical Review*, **147**, 295-302. https://doi.org/10.1103/PhysRev.147.295

[6] Bumgartner, T., *et al.* (2014) Effects of Neutron Irradiation on Pinning Force Scaling in State-of-the-Art Nb_3Sn Wires. *Superconductor Science and Technology*, **27**, Article ID: 015005. https://doi.org/10.1088/0953-2048/27/1/015005

[7] Jones, C.K., Hulm, J.K. and Chandrasekhar, B.S. (1964) Upper Critical Field of Solid Solution Alloys of the Transition Elements. *Reviews of Modern Physics*, **36**, 74-76. https://doi.org/10.1103/RevModPhys.36.74

[8] Gor'kov, L.P. (1960) The Critical Supercooling Field in Superconductivity Theory. *Soviet Physics JETP*, **37**, 593-599.

[9] Malik, G.P. and Varma, V.S. (2021) A New Microscopic Approach to Deal with the Temperature- and Applied Magnetic Field-Dependent Critical Current Densities of Superconductors. *Journal of Superconductivity and Novel Magnetism*, **34**, 1551-1561. https://doi.org/10.1007/s10948-021-05852-8

[10] Gordon, E.E., *et al.* (2016) Structure and Composition of the 200 K-Supercon Ducting Phase of H_2S at Ultrahigh Pressure: The Perovskite (SH^-) (H_3S^+). *Angewandte Chemie International Edition*, **55**, 3682-3684. https://doi.org/10.1002/anie.201511347

[11] Talantsev, E.F. (2020) Deby Temperature in LaHx-LaDy Superconductors. arXiv: 2004.03155.

[12] Malik, G.P. (2021) The Debye Temperatures of the Constituents of a Composite Superconductor. *Physica B: Condensed Matter*, **628**, Article ID: 413559. https://doi.org/10.1016/j.physb.2021.413559

[13] Malik, G.P. (2016) Superconductivity: A New Approach Based on the Bethe-Salpeter Equation in the Mean-Field Approximation. World Scientific Publishing Co Pte Ltd, Singapore. https://doi.org/10.1142/9868

[14] Gor'kov, L.P. and Kresin, V.Z. (2018) Colloquium: High Pressure and Road to Room Temperature Superconductivity. *Reviews of Modern Physics*, **90**, Article ID: 011001. https://doi.org/10.1103/RevModPhys.90.011001

[15] Malik, G.P. and Varma, V.S. (2022) On the Temperature- and Magnetic Field-Dependent Critical Current Density of Compressed Hydrogen Sulphide. *Journal of Superconductivity and Novel Magnetism*, **35**, 3119-3126. https://doi.org/10.1007/s10948-022-06357-8

[16] Hirsch, J.E. and Marsiglio, F. (2022) Clear Evidence against Superconductivity in Hydrides under High Pressure. *Matter and Radiation at Extremes*, **7**, Article ID: 058401. https://doi.org/10.1063/5.0091404

[17] Dogan, M. and Cohen, M.L. (2021) Anomalous Behavior in High-Pressure Carbonaceous Sulfur Hydride. *Physica C: Superconductivity and Its Applications*, **583**, Article ID: 1353851. https://doi.org/10.1016/j.physc.2021.1353851

[18] Malik, G.P., Malik, U., Pande, L.K. and Varma, V.S. (1995) On Solar Emission Lines: Calculation of Relative Line Intensities Based on the Finite-Temperature Schroedinger Equation. *Astrophysical Journal*, **447**, Article 443. https://doi.org/10.1086/175888

[19] Malik, G.P., Jha, R.K. and Varma, V.S. (1998) Quarkonium Mass Spectra from the Temperature Dependent Bethe-Salpeter Equation with Logarithmic and Coulomb plus Square-Root Kernels. *The European Physical Journal A—Hadrons and Nuclei*, **3**, 373-375. https://doi.org/10.1007/s100500050191